applied sciences

MDPI

Article

Characterization and Comparative Analysis of Mechanical Parameters of FDM- and SLA-Printed ABS Materials

Elvis Hozdić

Faculty of Mechanical Engineering, University of Novo mesto, Na Loko 2, 8000 Novo Mesto, Slovenia; elvis.hozdic@fs-unm.si

Abstract: This research paper provides an in-depth examination of the mechanical characteristics of 3D-printed specimens made from acrylonitrile butadiene styrene (ABS) and resins akin to ABS, with a focus on two widely used 3D printing methodologies: fused deposition modeling (FDM) and stereolithography (SLA). The study investigates how variations in 3D printing technology and infill density impact mechanical parameters such as Young's modulus, tensile strength, strain, nominal strain at break, maximum displacement, and maximum force at break. Tensile testing was conducted to assess these critical parameters. The results indicate distinct differences in mechanical performance between FDM- and SLA-printed specimens, with SLA consistently showing superior mechanical parameters, especially in terms of tensile strength, displacement, and Young's modulus. SLA-printed specimens at 30% infill density exhibited a 38.11% increase in average tensile strength compared to FDM counterparts and at 100% infill density, a 39.57% increase was observed. The average maximum displacement for SLA specimens at 30% infill density showed a 14.96% increase and at 100% infill density, a 30.32% increase was observed compared to FDM specimens. Additionally, the average Young's modulus for SLA specimens at 30% infill density increased by 17.89% and at 100% infill density, a 13.48% increase was observed, highlighting the superior mechanical properties of SLA-printed ABS-like resin materials. In tensile testing, FDM-printed specimens with 30% infill density showed an average strain of 2.16% and at 100% infill density, a slightly higher deformation of 3.1% was recorded. Conversely, SLA-printed specimens at 30% infill density exhibited a strain of 2.24% and at 100% infill density, a higher strain value of 4.15% was observed. The comparison suggests that increasing the infill density in FDM does not significantly improve deformation resistance, while in SLA, it leads to a substantial increase in deformation, raising questions about the practicality of higher infill densities. The testing data underscore the impact of infill density on the average nominal strain at break, revealing improved performance in FDM and significant strain endurance in SLA. The study concludes that SLA technology offers clear advantages, making it a promising option for producing ABS and ABS-like resin materials with enhanced mechanical properties.

Keywords: additive manufacturing; FDM; SLA; ABS filament; ABS resin; mechanical parameters

check for updates

Citation: Hozdić, E. Characterization and Comparative Analysis of Mechanical Parameters of FDM- and SLA-Printed ABS Materials. *Appl. Sci.* **2024**, *14*, 649. https://doi.org/10.3390/app14020649

Academic Editors: Tze Chuen Yap, Kean How Cheah and Mohd Rizal Alkahari

Received: 12 December 2023
Revised: 28 December 2023
Accepted: 10 January 2024
Published: 12 January 2024

Copyright: © 2024 by the author. Licensee MDPI, Basel, Switzerland. This article is an open access article distributed under the terms and conditions of the Creative Commons Attribution (CC BY) license (https://creativecommons.org/licenses/by/4.0/).

1. Introduction

Additive manufacturing (AM) [1–4] has become extensively popular and marks a considerable transformation in the manufacturing sector.

The F42 International Committee from the American Society for Testing and Materials (ASTM) provides a detailed description of additive manufacturing (AM). They define it as an innovative process that combines materials to create objects straight from 3D computer models. Distinctly, this method builds objects layer by layer, which is a significant shift away from traditional subtractive manufacturing methods [5]. The result is a more efficient and versatile manufacturing paradigm that opens the door to an array of new possibilities.

According to the ISO/ASTM 52900:2015 standard [6], additive manufacturing (AM) technologies are classified into distinct categories based on their operational principles. This classification system, as referenced in sources [3,7,8], organizes the technologies into broad

groups, each defined by its unique approach to material manipulation and deposition, ranging from jetting and photopolymerization processes to fusion and lamination techniques.

Additionally, based on the kind of base material utilized, additive manufacturing (AM) can be classified into three groups: technologies based on solid, liquid, and powder materials [9]. These technologies encompass laminated object manufacturing (LOM), fused deposition modeling (FDM), selective laser sintering (SLS), stereolithography (SLA), 3D plotting, direct energy deposition (DED), InkJet printing (IJP), direct write (DW), etc.

For this study, the technologies of FDM and SLA were chosen. FDM is recognized as a broadly utilized and easily accessible method in the field of additive manufacturing for 3D printing, as supported by numerous research findings [10–14]. In the realm of FDM, the process unfolds with the melting of thermoplastic filaments, which are then meticulously deposited, layer by layer.

The FDM process operates by extruding a plastic material (filament) through an extruder, typically positioned at the rear of the 3D printer. In the FDM process, a pulley-drive system within the extruder pushes the filament into a heated nozzle at a controlled rate. The nozzle, part of the extruder or print head, features resistive heaters that maintain the filament's temperature slightly above its glass transition point, rendering it in a semi-liquid state. This molten filament is then extruded smoothly through the nozzle onto a build platform. Upon extrusion, it rapidly reverts to its solid state, shaping the desired pattern. This iterative process continues until the model is complete, at which point it is removed from the build chamber for post-processing [14,15].

FDM technology is characterized by its ability to utilize a diverse range of thermoplastic substances. This includes materials such as acrylonitrile butadiene styrene (ABS), acrylonitrile styrene acrylate (ASA), polyamide (PA), polylactide (PLA), and polyethylene terephthalate glycol-modified (PETG), as highlighted in source [16]. This versatility empowers users to select materials that align with their unique product needs. The wide array of available materials enables the manufacturing of products with diverse attributes, including qualities such as strength, flexibility, and resistance to temperature and chemicals.

The SLA is a technology for rapid prototyping and 3D printing that focuses on using ultraviolet (UV) rays to cure liquid resin and create three-dimensional objects layer by layer [17–23]. This technology represents one of the earliest methods for 3D printing and continues to be essential for producing accurate and top-quality models and products. The method ensures enhanced precision in component dimensions, exceptional quality in surface finish, and beneficial mechanical properties [19].

The SLA printing process commences with a 3D model of the intended product. The printer systematically applies a layer of resin to the work surface and solidifies it using directed UV light. This layer-by-layer solidification process is repeated until the entire product is finished. Following the printing, an additional UV light exposure is often required to ensure full solidification [19].

Three-dimensionally-printed objects can undergo UV curing to enhance the solidification process [20]. UV exposure prompts the creation of additional chemical bonds, enhancing the resin's mechanical strength and stability. Parameters like temperature, wavelength, and curing time used during the process impact the ultimate properties [20]. Additionally, this curing method can enhance product homogeneity.

SLA technology allows for exceptionally precise printing with high resolution, meaning that printed products are highly detailed and have smooth surfaces. There is a wide range of different materials that can be used in SLA printing, including transparent, solid, flexible, engineering, and even medical resins (biocompatible resins, dental resins, etc.).

In this study, FDM and SLA printers were used to manufacture ABS and ABS-like specimens for mechanical testing.

ABS is a copolymer that exhibits a unique chemical composition composed of three primary monomers: acrylonitrile (15% to 35%), butadiene (5% to 30%), and styrene (40% to 60%) [24–26]. Each of these monomers contributes distinct properties to the polymer, which collectively result in ABS's exceptional characteristics.

Based on the review of the scientific literature [27–46], it can be concluded that the mechanical properties of FDM 3D-printed ABS polymer materials have been explored from various perspectives, such as the impacts of the raster angle [31–34], layer thickness [35–37], infill percentage [38–41], printing speed [42–44], etc.

In the paper [38], Baich et al. examined how varying infill percentages impacted the mechanical strength and production costs of 3D-printed ABS components. They conducted experiments with infill percentages set at 50%, 75%, and 100%. Their findings revealed that components created with 100% infill consistently exhibited superior mechanical properties when compared to those with 50% infill.

Yadav et al. [39] explore the effects of infill density, material density, and extrusion temperature on the mechanical characteristics of ABS, PETG, and multi-material samples produced through FDM printing in their study. They create multi-material specimens by alternately layering 50% ABS and 50% PETG using FDM 3D printing. The researchers emphasize that the ultimate tensile strength (UTS) experiences a 20% increase when the infill proportion is raised from 20% to 60%.

Samykano et al. [40] investigated how various printing parameters, such as the infill percentage, affect the mechanical properties of ABS printed using FDM. They also developed a mathematical model for the numerical prediction of these properties, employing response surface methodology. Their research showed notable enhancements in both tensile strength and Young's modulus correlating with an increase in infill percentage.

In the paper [41], the authors determined that raising the infill percentage from 20% to 50% in ABS results in a 26% enhancement in ultimate tensile strength (UTS), a 24% increase in yield stress, a 45% boost in Young's modulus, and a slight 1% improvement in elongation at break.

ABS-like resin is part of the group of thermoplastic polymers consisting of three components: acrylonitrile, butadiene, and styrene [47–53]. As reported in [49], the presence of acrylonitrile enhances the thermal and chemical resilience, along with the surface hardness of the end product. Meanwhile, butadiene plays a crucial role in augmenting the toughness and impact resistance, whereas styrene is instrumental in improving processability, rigidity, and the overall strength of the material.

ABS-like resins are well-suited for 3D printing components that require moderate detailing, high durability, and adequate functionality [50]. ABS-like resins are highly regarded in the industrial sector for their adaptability and superior characteristics. Often utilized in 3D printing, these resins enable the production of components with decent detailing, robust strength, and effective functionality. Their extensive utilization encompasses the fabrication of computer consoles, domestic materials, components for both the interior and exterior of vehicles, luggage items, and a variety of piping systems [54].

ABS-like resin material is accessible for commercial purposes; however, it lacks extensive mechanical research, resulting in limited available literature [47]. In the paper [47], Golubović et al. conducted an extensive mechanical examination of both ABS and similar polymers produced via additive manufacturing techniques such as FDM, SLA, and DLP. The research utilized test samples with a complete infill density and a print orientation of 90 degrees. The mechanical characteristics were evaluated using tests for tensile strength, bending, and compression, as well as analyses of the morphology, size precision, and Shore A hardness. The outcomes of the tensile experiments revealed that the toughness offered by the FDM technique constitutes roughly 40% of that attained through DLP, with the elongation at break in FDM reaching 37% of DLPs. Furthermore, the ultimate tensile stress of SLA was observed to surpass that of FDM by an estimated 27%.

As highlighted through a review of the relevant scientific literature, ABS filaments have been well-researched through various mechanical tests. However, in the case of ABS-like resin, the author of this article notes and identifies a scientific gap in this domain. Various factors influence the final product's quality, making continuous material testing in different 3D printing processes crucial.

Drawing from the author's expertise in the domain, there appears to be an absence of systematic comparative studies in the scientific literature that evaluate the mechanical characteristics and properties of ABS materials printed with FDM and SLA techniques, particularly focusing on varying infill densities (30% and 100%) in the samples. Key benefits of incorporating infill in 3D-printed objects are the reduction in material usage, decreased weight of the final product, and acceleration of the manufacturing process, all of which significantly influence the overall cost of the end product.

This study aims to address this gap by investigating and comparing the mechanical parameters of ABS materials (ABS filament and ABS-like resin) produced through two popular 3D printing technologies, FDM and SLA. Variations in 3D printing technology and infill density can significantly impact the mechanical properties of ABS materials, which is crucial for industries relying on these materials, affecting product safety and durability.

In this research, the researcher selected 30% and 100% as the infill density benchmarks for evaluating the mechanical characteristics of ABS materials. Using 100% infill density allows for an effective comparison between the mechanical properties of the test samples and the manufacturer's specifications for ABS materials. The choice of 30% density is based on a thorough examination of the existing scientific literature, serving as an additional standard for assessment.

The focus of this research is on examining how changes in 3D printing techniques and infill density influence crucial mechanical properties, such as Young's modulus, tensile strength, strain, the nominal strain at break, peak displacement, and the highest force at break. The method of tensile testing was used to assess these essential parameters.

The research also includes a comparative analysis of the measured mechanical parameters against the manufacturer's specifications for ABS materials. The findings show significant disparities in mechanical efficacy between specimens printed using FDM and SLA techniques. Notably, SLA-printed samples exhibited enhanced mechanical properties, especially in terms of tensile strength, displacement, and Young's modulus.

The analysis implies that a higher infill density in FDM printing does not markedly enhance resistance to deformation. Conversely, in SLA printing, a greater infill density results in a notable increase in deformation, prompting queries regarding the effectiveness of using higher infill densities in practical applications.

2. Materials, Methods, and Equipment

2.1. Material Specification

For this paper, two commercially material types, ABS filament (PlastikaTrček, Ljubljana, Slovenia) and ABS-like resin (Anycubic, Hongkong, China), were used.

The specifications and mechanical parameters of ABS filament and ABS-like resin according to the manufacturers are presented in Tables 1–3 [55,56].

Table 1. ABS filament specification [55].

Parameter	Value
Diameter (mm)	1.75
Colour	black
Extrusion temperature (°C)	240–260
Bed platform temperature (°C)	90–120
Printing speed (mm/s)	40–120
Layer height (mm)	0.1–0.2

Table 2. ABS-like resin specification [56].

Parameter	Value
Layer thickness (mm)	0.05
Colour	silver
Normal exposure time (s)	2–3
Off time (s)	0.5–2
Bottom exposure time (s)	20–40
Bottom layers	3–6
Z lift distance (mm)	5–10
Z lift speed (mm/s)	2–6
Z retract speed (mm/s)	2–6

Table 3. Mechanical parameters of ABS filament [55] and ABS-like resin [56].

Material Type	ABS Filament	ABS-like Resin
Density (g/cm^3)	1.04	1.05–1.25
Tensile strength (MPa)	≥43	35–55
Flexural strength (MPa)	≥65	50–60
Young's modulus (MPa)	≥2100	1400–1600
Elongation at break (%)	≥30	30–40

Table 3 presents mechanical parameters sourced from the filament manufacturer [55] corresponding to the test samples with a complete 100% infill density.

The research employed filaments of a circular cross-section, conforming to the manufacturer's specifications [55], characterized by an average diameter of 1.75 mm and demonstrating minimal standard deviation.

2.2. Specimens Geometrical Dimensions, Manufacturing Parameters, and Experimental Procedures

The empirical investigation involved the use of SolidWorks 2020, a 3D CAD software, for the design and creation of the test specimens. SolidWorks 2020 was utilized to design the model of the tensile test specimen, in compliance with the ISO 527-2:2012 standard [57], as depicted in Figure 1.

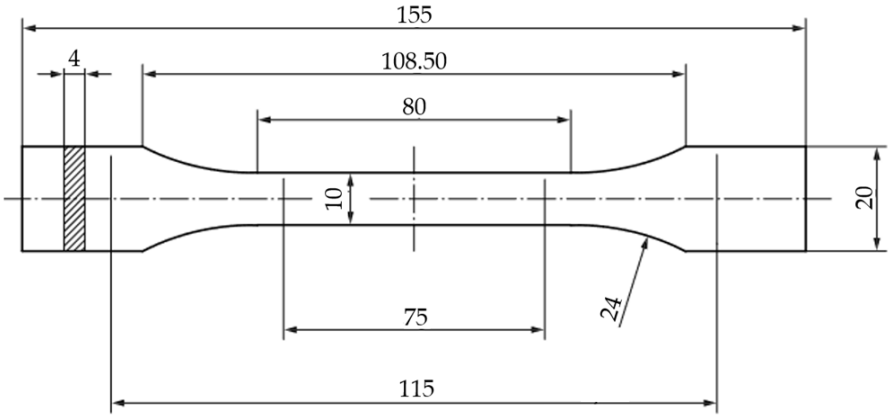


Figure 1. Design of the tensile test specimen following the guidelines of the ISO 527-2:2012 standard.

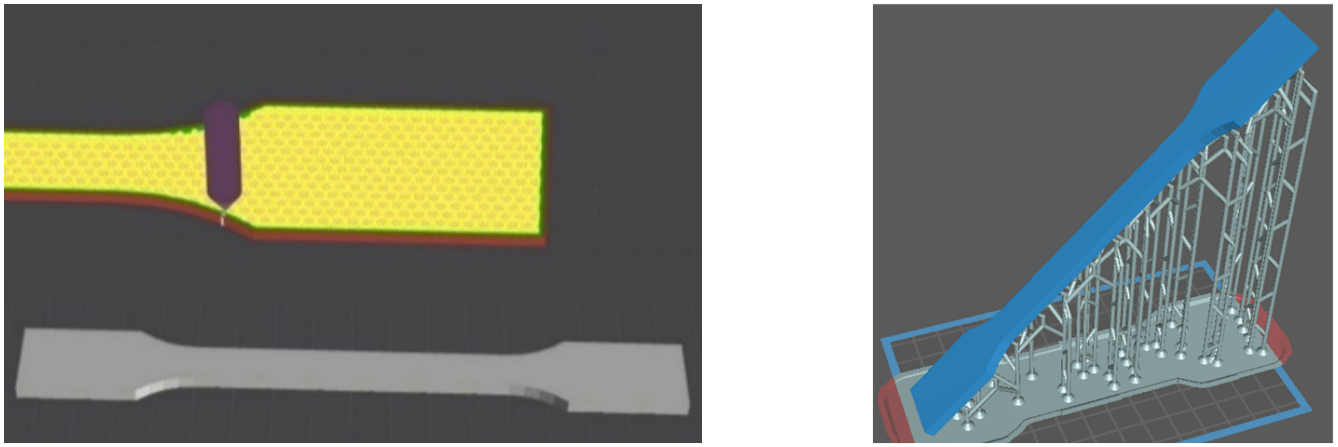
Subsequently, the models designated for tensile testing were transformed into the STL file format. These files serve as the foundational input for configuring and fine-tuning the parameters within the 3D printing workflow.

The Creality K1 3D printer (Creality, Shenzhen, China), utilizing FDM technology, and the HALOT-MAGE PRO 8K Resin 3D Printer (Creality, Shenzhen, China), employed for SLA technology, were utilized in the fabrication of the tensile test specimens.

The printer parameters were adjusted using the Creality slicer software (v. 4.3.8.6984) for the FDM 3D printer (https://wiki.creality.com/en/Software-&-Firmware/Creality-

Slicing-Software/new-page/, accessed on 17 October 2023) and the ChituBox slicer (Version 1.9.5) for the SLA 3D printer (https://www.chitubox.com/en/download/chitubox-free, accessed on 2 December 2023).

Within the Creality slicer software, users can choose from four infill patterns: line, hexagon, triangle, and 3D infill. In this research, the 'Hexagon' infill pattern was consistently applied to all ABS tensile test samples, utilizing both 30% and 100% fill densities, as illustrated in Figure 2a.



(**a**) (**b**)

Figure 2. Specimen with "Hexagon" infill pattern: (**a**) in Creality slicer software and (**b**) in ChituBox slicer software.

Upon configuring the requisite parameters in the Creality slicer software, as elaborated in Table 4, G-code was produced and then forwarded to the computer overseeing the 3D printer's operations.

Table 4. Main FDM 3D-printing parameters.

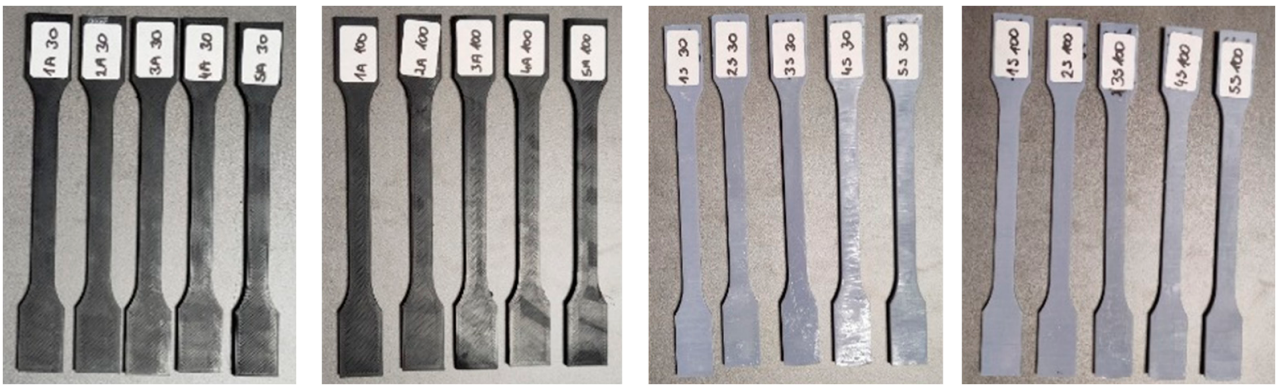
Parameter	Value
Filament diameter (mm)	1.75
Infill pattern	Hexagon
Infill density (%)	30; 100
Nozzle diameter (mm)	0.40
Base print speed (mm/s)	300.00
Travel speed (mm/s)	500.00
First layer maximum (mm/s)	60.00
Top solid layers	3
Bottom solid layers	3
Layer height (mm)	0.15
First layer height (mm)	0.15
Extrusion temperature (°C)	250
Bed temperature (°C)	90

The configuration of parameters for the SLA 3D printer was performed in the ChituBox slicer software (Version 1.9.5), as shown in Table 5. In Figure 2b, ABS-like tensile test specimens are displayed, employing a "Hexagon" infill pattern with fill densities of both 30% and 100%.

Table 5. Main SLA 3D-printing parameters.

Parameter	Value
Infill pattern	Grid3D
Infill density (%)	30; 100
Top solid layers	3
Bottom layers	3
Layer thickness (mm)	0.1
Bootom exposure time (s)	25
Normal exposure time (s)	2
Z lift distance (mm)	5
Z lift speed (mm/s)	4
Z retract speed (mm/s)	4
Laser beam size (mm)	0.08
Printing orientation (°)	45

A total of 20 identical tensile test specimens were printed, with ten specimens produced for each material (Figure 3).



(**a**) (**b**) (**c**) (**d**)

Figure 3. Three-dimensionally-printed ABS and ABS-like specimens: (**a**) ABS with 30% fill density (FDM), (**b**) ABS with 100% fill density (FDM), (**c**) ABS-like with 30% fill density (SLA), and (**d**) ABS-like with 100% fill density (SLA).

Table 6 exhibits the recorded parameters during the 3D printing process of all ABS and ABS-like tensile specimens. The printing was conducted using both the Creality K1 3D printer and the Geetech Alkaid 2K mono LCD screen printer.

Table 6. Recorded parameters during the 3D printing.

Recorded Parameter	Infill Density	ABS Filament	ABS-like Resin
Print time (h.min.s)	30%	00.23.14	06.38.14
	100%	00.26.42	06.38.14
Material mass used (g)	30%	8.00	21.60
	100%	9.00	24.60
Filament length used (m)	30%	4.01	-
	100%	3.62	-
Quantity of material used (mL)	30%	-	19.63
	100%	-	22.31

All the 3D-printed specimens underwent testing in compliance with the ISO 527-2:2012 standard. The tensile examinations were performed utilizing the Zwick Z 100 universal testing machine (Zwick-Roell, Ulm, Germany), equipped with a maximum load capacity of 100 kN and a testing velocity of 5 mm/min.

The gathered data encompass the specimens tested and their respective tensile test results. The testXpert software (Version II) was employed for the collection and supervision of the tensile test data. This advanced software enables not only the acquisition of key data points such as the tensile strength (σ in MPa), strain (ε in %), nominal strain at break (ε_{tb} in %), and Young's modulus (E in MPa) for each test but also assists in generating tensile strength–strain curves.

Subsequently to the tensile strength data being obtained, the forthcoming section will detail the results, which were processed using Excel. The mechanical parameters, specifically the maximum displacement (ΔL in mm) and the maximal force at break (F_{max} in N), were determined based on the data from the tensile tests.

The maximal displacement, denoted as ΔL, was calculated utilizing Equation (1), wherein ε signifies the nominal strain at break and L corresponds to the initial grip separation, as depicted in Figure 4. Concurrently, the maximal force at break, F_{max}, was ascertained using Equation (2). In this equation, E is Young's modulus, A indicates the narrowest cross-sectional area, ΔL is the maximal displacement, and L is the initial grip separation distance.

$$\Delta L = \varepsilon \cdot L \cdot \frac{1}{100\%} \tag{1}$$

$$F_{\max} = E \cdot A \cdot \frac{\Delta L}{L} \tag{2}$$

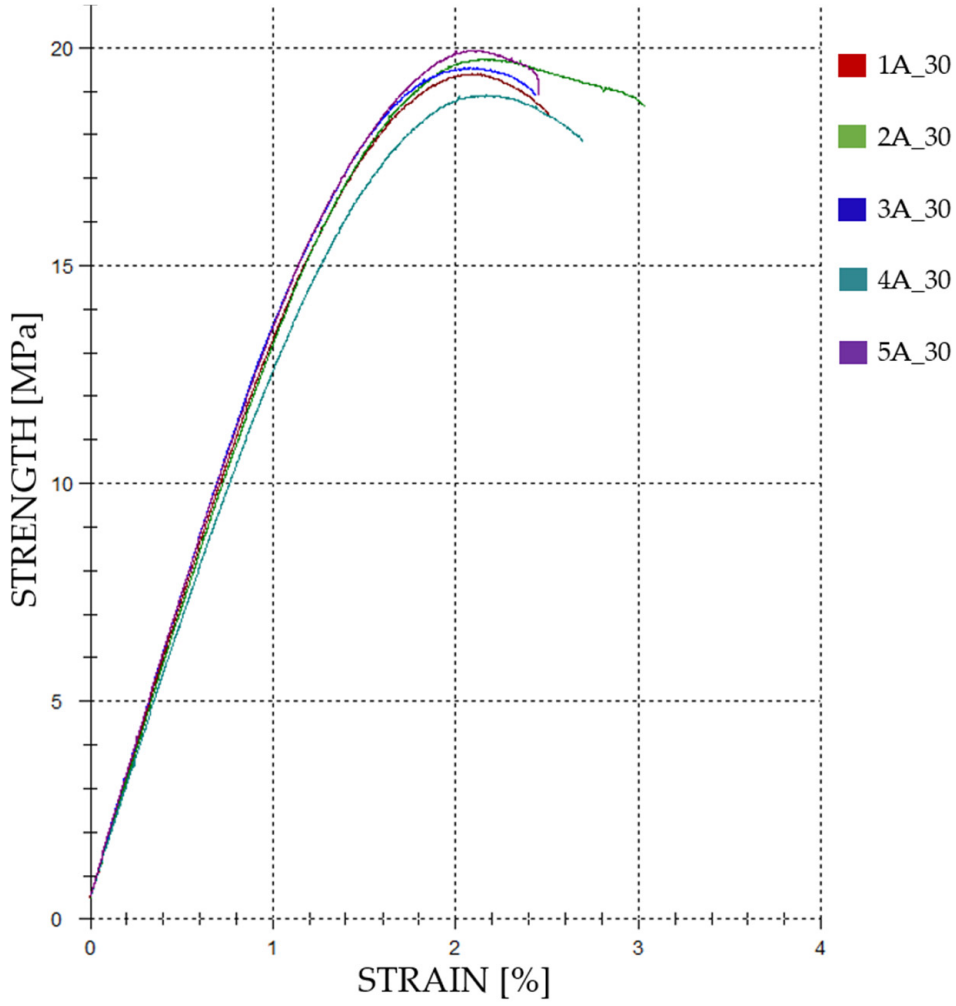


Figure 4. The tensile strength–strain curves for ABS specimens produced using FDM 3D printing with a 30% infill density (referred to as Case 1).

The following section will showcase the outcomes derived from evaluating the tensile mechanical properties of 3D-printed specimens using ABS filament and ABS-like resin.

The data from the tensile tests are categorized into four distinct sections: (1) information from FDM 3D-printed ABS samples made with ABS filament and 30% infill density (1A_30, 2A_30, 3A_30, 4A_30, and 5A_30)—referred to as Case 1, (2) details of FDM 3D-printed ABS samples produced with ABS filament and 100% infill density (1A_100, 2A_100, 3A_100, 4A_100, and 5A_100)—known as Case 2, (3) data from SLA 3D-printed ABS-like samples created using ABS-like resin with 30% infill density (1S_30, 2S_30, 3S_30, 4S_30, and 5S_30)—termed Case 3, and (4) information on SLA 3D-printed ABS-like samples made from ABS-like resin with a 100% infill density (1S_100, 2S_100, 3S_100, 4S_100, and 5S_100)—designated as Case 4.

3. Results

3.1. Mechanical Properties of the FDM 3D-Printed and Tensile-Tested ABS Specimens

The tensile test data for all FDM 3D-printed ABS specimens are shown in Table 7.

Table 7. FDM 3D-printed ABS tensile-tested specimens: test results.

Case	Specimen Code	Tensile Strength σ [MPa]	Strain ε [%]	Nominal Strain at Break ε_{tB} [%]	Young's Modulus E [MPa]
Case 1	1A_30	19.423	2.11	2.51	1376.824
	2A_30	19.756	2.15	3.13	1138.182
	3A_30	19.545	2.14	2.42	1409.644
	4A_30	18.911	2.22	2.76	1278.181
	5A_30	19.912	2.17	2.54	1400.937
	Average (St. Dev.)	19.509 (0.384)	2.16 (0.04)	2.67 (0.28)	1320.754 (114.695)
Case 2	1A_100	26.715	2.33	4.75	1730.422
	2A_100	28.635	2.26	3.22	1831.286
	3A_100	27.187	2.28	3.09	1751.838
	4A_100	27.545	2.13	3.11	1920.691
	5A_100	26.925	2.20	3.92	1788.691
	Average (St. Dev.)	27.401 (0.756)	2.24 (0.08)	3.62 (0.72)	1804.586 (75.380)

The graphical presentations of the tensile strength and strain for individual FDM 3D-printed ABS tensile-tested specimens are shown in Figures 4 and 5.

Figure 4 illustrates the graphical representation of the tensile test outcomes for FDM 3D-printed ABS samples with a 30% fill density (referred to as Case 1), whereas Figure 5 shows the results of tensile tests for ABS samples with a 100% fill density (identified as Case 2).

The examination of the graphs in Figure 4, combined with the mechanical parameters detailed in Table 7, clearly indicates that FDM 3D-printed ABS samples with a 100% infill density exhibit enhanced tensile strength and higher values for nominal strain at break.

The average value of the tensile strength increased by 28.81% in FDM 3D-printed ABS specimens with 100% infill density (Table 7 and Figure 6a).

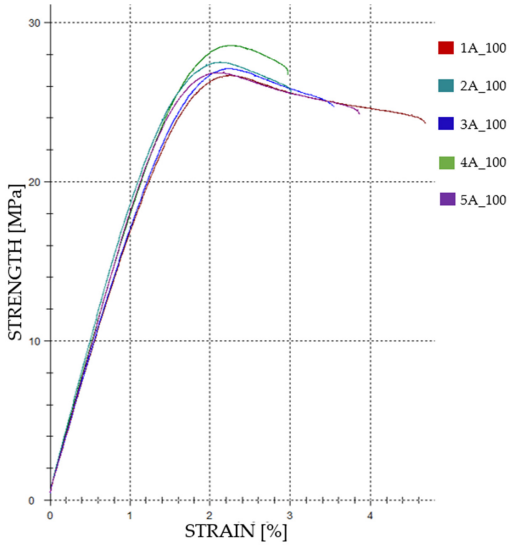


Figure 5. The tensile strength–strain curves for ABS specimens produced using FDM 3D printing with a 100% infill density (referred to as Case 2).

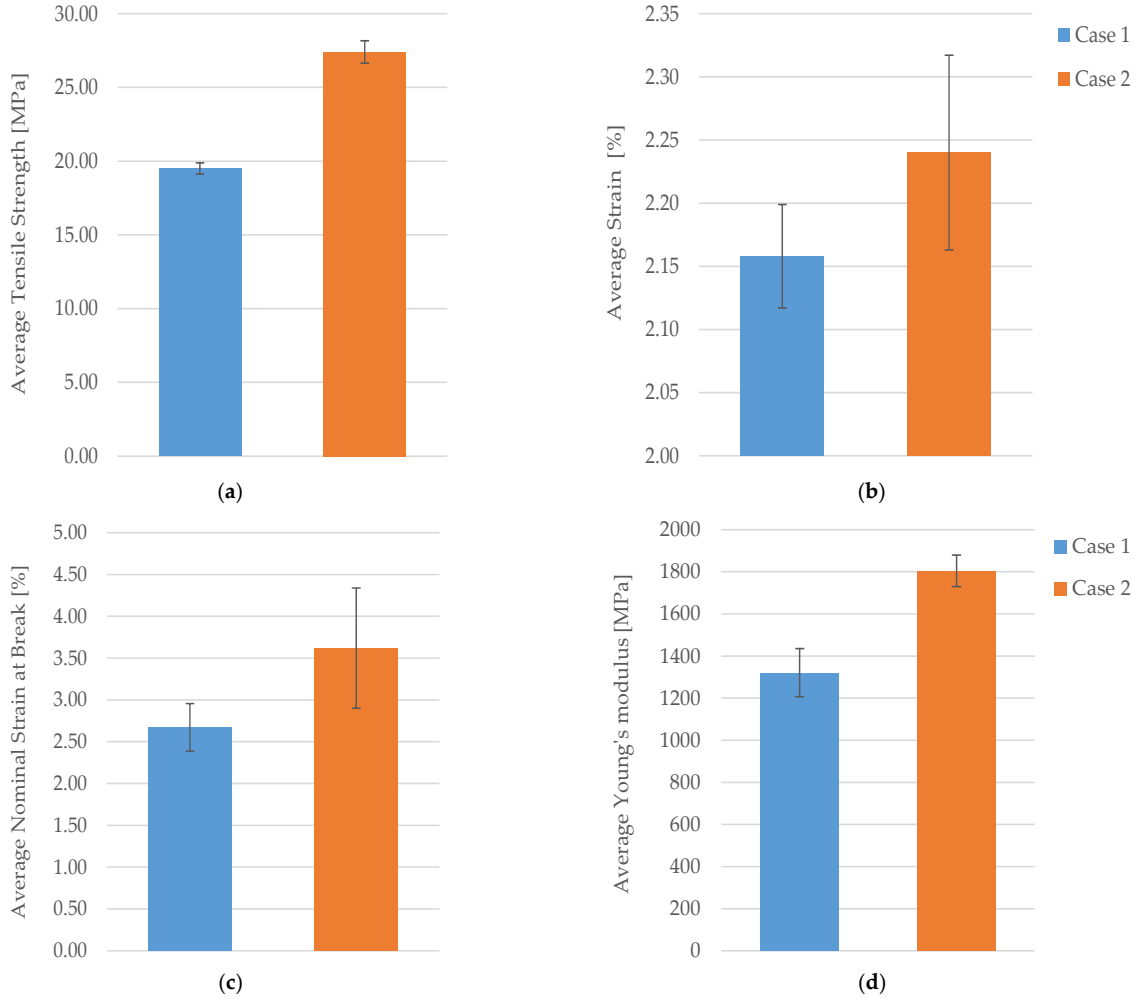


Figure 6. The mechanical parameters of ABS 3D-printed specimens using FDM were tested under tensile loading conditions at two different infill densities: 30% (Case 1) and 100% (Case 2): (**a**) average tensile strength, (**b**) average strain, (**c**) average nominal strain at break, (**d**) average Young's modulus.

The average value of the strain increased by 3.57% in FDM 3D-printed ABS material specimens with 100% infill density compared to FDM 3D-printed ABS material specimens with 30% infill density (Table 7 and Figure 6b).

The impact of infill density on the efficacy of ABS specimens produced via FDM 3D printing is distinctly evident in both the average nominal strain at break and the average Young's modulus, as demonstrated in Figure 6.

The average nominal strain at break is 26.24% greater in FDM 3D-printed ABS specimens tested for tensile strength with 100% infill density when compared to specimens with 30% infill density (Figure 6c).

The average Young's modulus exhibited a similar pattern, as shown in Figure 6d. The average Young's modulus was 26.81% lower in FDM 3D-printed ABS specimens tested for tensile strength with 30% infill density compared to those with 100% infill density.

By employing the tensile test data showcased in Table 7 and applying Equations (1) and (2), the maximum force at break and the maximum displacement were calculated for the ABS specimens fabricated through FDM 3D printing and subjected to tensile testing. Table 8 and Figure 7 exhibit the respective average maximum displacement and average maximum force at break.

Table 8. The calculated value of mechanical parameters for FDM 3D-printed ABS tensile-tested specimens.

Case	Specimen Code	Max. Displacement ΔL [mm]	Max. Force at Break F_{max} [N]
Case 1	1A_30	2.89	794.750
	2A_30	3.60	822.497
	3A_30	2.78	817.702
	4A_30	3.17	771.801
	5A_30	2.92	825.025
	Average (St. Dev.)	3.07 (0.33)	806.355 (22.729)
Case 2	1A_100	5.46	1177.557
	2A_100	3.70	1217.823
	3A_100	3.55	1198.283
	4A_100	3.58	1194.612
	5A_100	4.51	1181.455
	Average (St. Dev.)	4.16 (0.83)	1193.946 (15.922)

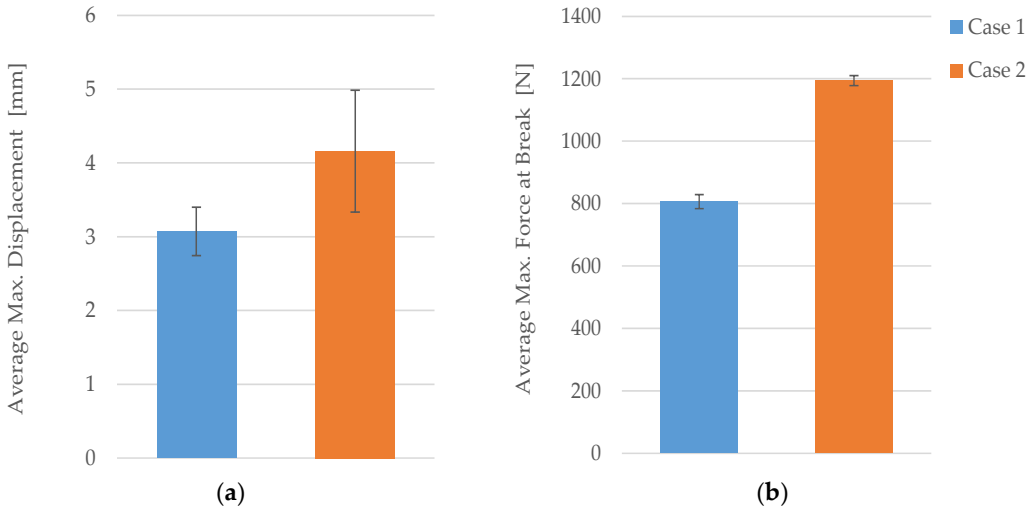


Figure 7. The calculated average value of mechanical parameters for FDM 3D-printed ABS tensile-tested specimens: (**a**) average maximal displacement and (**b**) average maximal force at break.

Based on the data from Table 8, it is evident that the average maximal displacement value increased by 35.51% in FDM 3D-printed ABS specimens with 100% infill density compared to ABS specimens with 30% infill density (Figure 7a). Furthermore, the average value of the maximal force at break demonstrates a 26.29% increase, as depicted in Figure 7b.

When contrasting the average tensile strengths of the FDM 3D-printed ABS specimens with a 100% infill density against the manufacturer's specified values for ABS filament, it is evident that these FDM 3D-printed specimens achieve about 63.72% of the values indicated for the filament (Figure 8a).

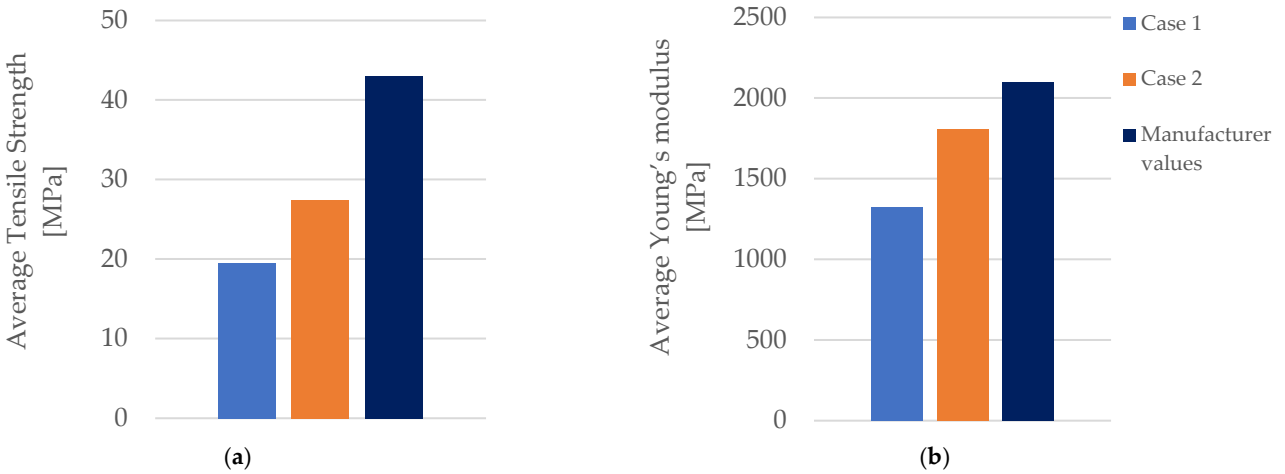


Figure 8. Comparison between tensile strength and Young's modulus of FDM 3D-printed ABS specimens post-tensile testing and manufacturer-specified filament values: (**a**) average tensile strength, (**b**) average Young's modulus.

Similarly, in analyzing Young's modulus, the juxtaposition of results from the FDM 3D-printed ABS specimens with 100% infill density and the manufacturer-specified values for ABS filament reveals that these FDM 3D-printed specimens attain roughly 85.92% of the filament's designated values (Figure 8b).

3.2. Mechanical Properties of the SLA 3D-Printed and Tensile-Tested ABS-like Resin Specimens

Table 9 presents the tensile testing data for all ABS-like resin specimens fabricated using SLA 3D printing. Figures 9 and 10 depict the graphical representations of tensile strength and strain for each of the ABS-like resin specimens subjected to tensile testing.

Figure 9 represents a graphical depiction of the tensile test results for SLA 3D-printed ABS-like resin tensile-tested specimens with 30% fill density (Case 3), while Figure 10 displays the tensile test results for ABS-like resin tensile-tested specimens with 100% fill density (Case 4).

Upon thorough examination of the graphs displayed in Figures 9 and 10, a clear pattern emerges. It is clearly evident that the ABS-like resin specimens, produced through SLA 3D printing with a 100% infill density, demonstrate a notable enhancement in both tensile strength and nominal strain at break values. This observed enhancement underscores the efficacy of SLA 3D printing when producing high-strength ABS-like resin components, thus demonstrating its potential for applications demanding superior mechanical properties.

The average value of the tensile strength exhibited a notable 30.49% increase in SLA 3D-printed ABS-like resin specimens with a full 100% infill density (Figure 11a). This substantial rise in tensile strength underscores the remarkable capacity of SLA 3D printing to enhance the mechanical performance of ABS-like resin components, making them not only stronger but also more robust and reliable in a wide range of engineering and manufacturing applications. This improved tensile strength can open up new possibilities for designing and producing parts that must withstand substantial loads and stresses with greater confidence.

Table 9. SLA 3D-printed ABS-like resin tensile-tested specimens: test results.

Case	Specimen Code	Tensile Strength σ [MPa]	Strain ε [%]	Nominal Strain at Break ε_{tB} [%]	Young's Modulus E [MPa]
Case 3	1S_30	33.312	3.01	3.07	1698.081
	2S_30	25.658	2.36	2.36	1340.203
	3S_30	35.591	3.27	3.31	1787.256
	4S_30	33.018	2.59	2.61	1783.058
	5S_30	30.008	4.28	4.33	1434.025
	Average (St. Deev.)	31.517 (3.830)	3.10 (0.75)	3.14 (0.76)	1608.525 (207.890)
Case 4	1S_100	45.621	4.53	5.66	2050.024
	2S_100	45.468	4.56	5.81	2043.581
	3S_100	42.915	3.91	6.25	2202.640
	4S_100	44.694	3.34	3.33	2073.162
	5S_100	48.010	4.42	4.91	2059.801
	Average (St. Dev.)	45.342 (1.839)	4.15 (0.52)	5.19 (1.15)	2085.842 (66.237)

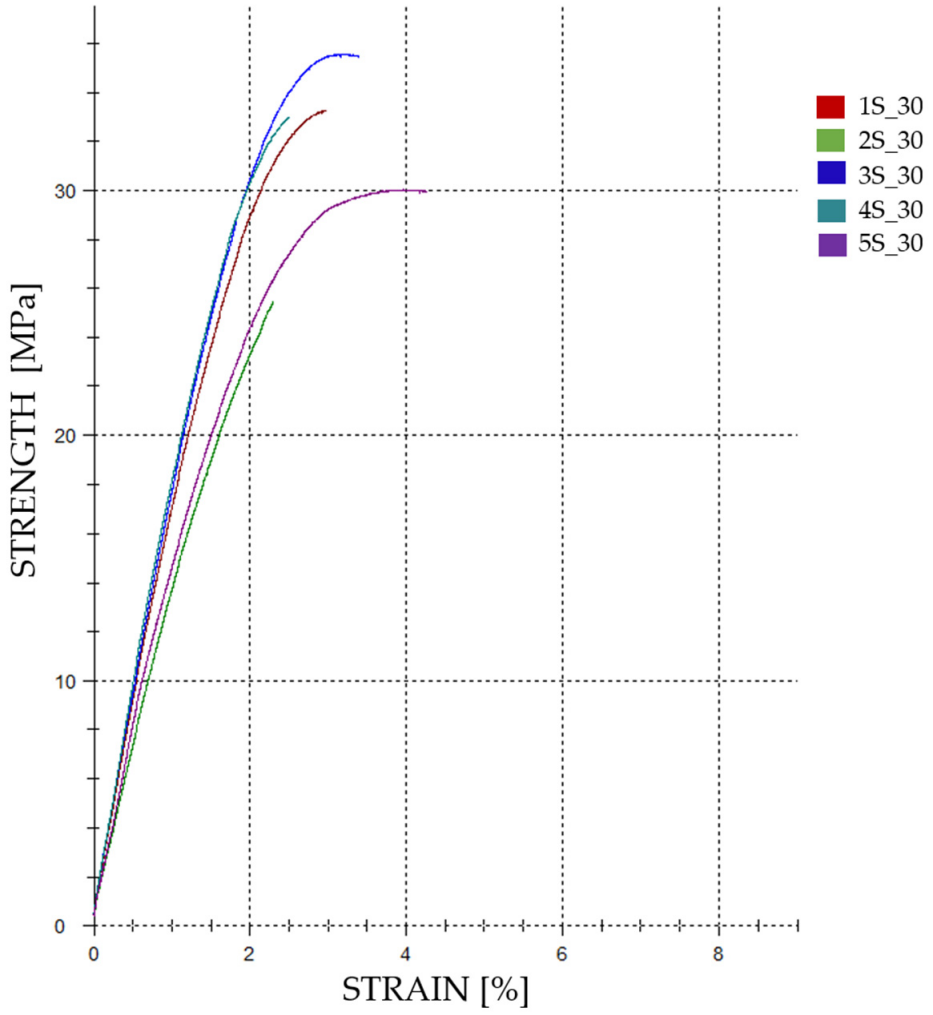


Figure 9. The tensile strength–strain curves for ABS-like resin specimens produced using SLA 3D printing with a 30% infill density (referred to as Case 3).

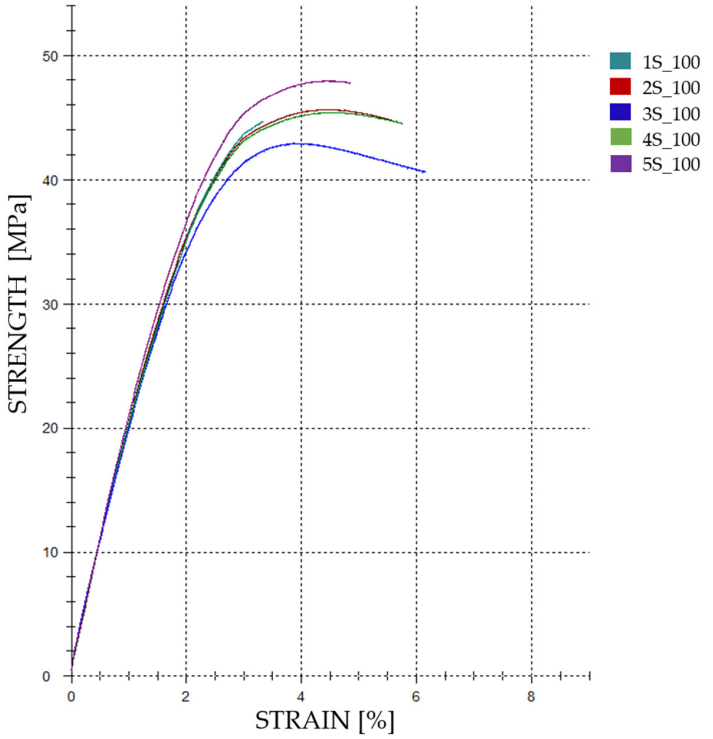


Figure 10. The tensile strength–strain curves for ABS-like resin specimens produced using SLA 3D printing with a 100% infill density (referred to as Case 4).

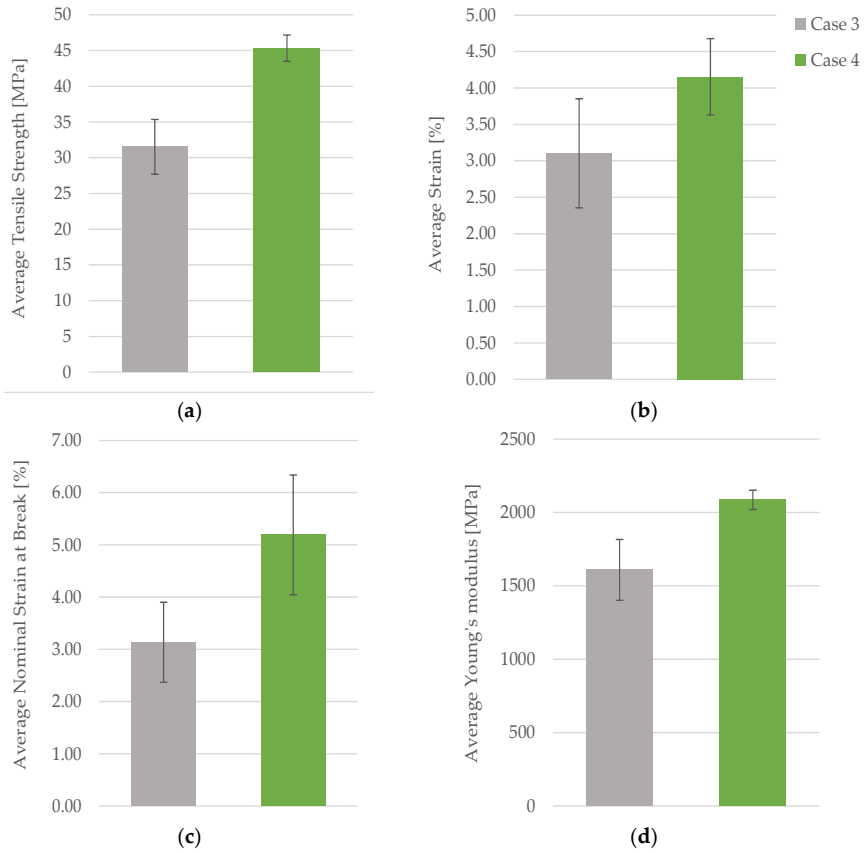


Figure 11. The mechanical parameters of SLA 3D-printed ABS-like resin tensile-tested specimens with 30% (Case 3) and 100% (Case 4) infill density: (**a**) average tensile strength, (**b**) average strain, (**c**) average nominal strain at break, (**d**) average Young's modulus.

The average strain value exhibited a 25.30% increase in SLA 3D-printed ABS material specimens with 100% infill density as opposed to those with 30% infill density (refer to Table 9 and Figure 11b).

The data emphasizes a substantial 25.30% rise in nominal strain at break for SLA 3D-printed ABS-like resin specimens with 100% infill density, in contrast to those with a 30% infill density, as illustrated in Figure 11c. This improvement underscores the heightened flexibility and durability achieved with higher infill densities in SLA 3D printing. This advancement has broad implications, particularly in applications requiring materials to endure deformation and stress without failing structurally. Components with full infill density exhibit greater resilience, allowing them to withstand more significant strains, thereby expanding their potential applications in engineering and design.

The same pattern was observed in the average Young's modulus, as depicted in Figure 11d. When examining SLA 3D-printed ABS-like resin samples, those with a 30% infill density exhibited an average Young's modulus that was 22.88% lower than that of SLA 3D-printed ABS-like resin specimens subjected to tensile testing, which had a 100% infill density.

Utilizing the data from Table 9 and applying Equations (1) and (2), the maximal displacement and maximal force at break for the SLA 3D-printed ABS-like resin specimens are calculated. The results for the average maximal displacement and average maximal force at break are presented in Table 10 and Figure 12.

Table 10. The calculated value of mechanical parameters for SLA 3D-printed ABS-like resin tensile-tested specimens.

Case	Specimen Code	Max Displacement ΔL [mm]	Max Force at Break F_{max} [N]
Case 3	1S_30	3.53	1374.599
	2S_30	2.71	1047.965
	3S_30	3.81	1433.605
	4S_30	3.01	1347.233
	5S_30	4.98	1238.802
	Average (St. Dev.)	3.61 (0.88)	1288.441 (151.859)
Case 4	1S_100	6.51	1845.802
	2S_100	6.67	1812.359
	3S_100	7.19	1709.733
	4S_100	3.83	1806.313
	5S_100	5.65	1924.241
	Average (St. Dev.)	5.91 (1.32)	1819.689 (77.36)

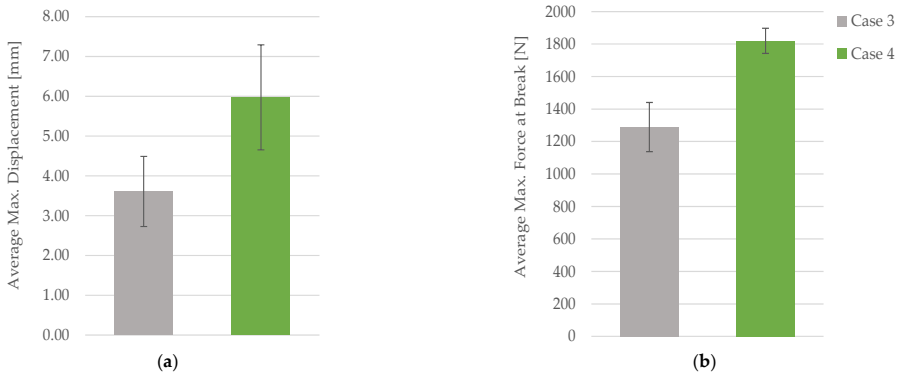


Figure 12. The calculated average value of mechanical parameters for SLA 3D-printed ABS-like resin tensile-tested specimens: (**a**) average maximal displacement and (**b**) average maximal force at break.

Based on the data presented in Table 10 and Figure 12, it is evident that the average maximum displacement exhibited a substantial increase of 38.92% in SLA 3D-printed ABS-like resin specimens with 100% infill density when compared to ABS-like resin specimens with 30% infill density (as depicted in Figure 12a). Additionally, as indicated in both Table 10 and Figure 12b, the average maximum force at the point of break decreased by 22.88% in Case 4 when compared to the value observed in Case 3.

Comparing the average tensile strengths, it is evident that the SLA 3D-printed ABS-like specimens with 100% infill density surpass the manufacturer's specified values for ABS-like resin by about 0.76%, as demonstrated in Figure 13a.

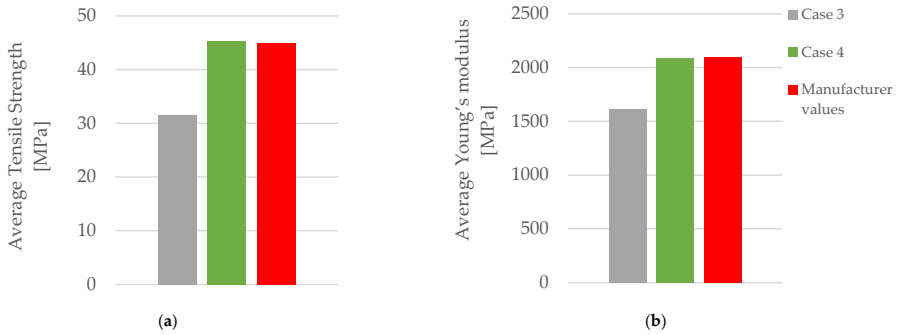


Figure 13. Comparison of the tensile strength and Young's modulus of the SLA 3D-printed ABS-like tensile-tested specimens with those of the resin (manufacturer values): (**a**) average tensile strength, (**b**) average Young's modulus.

Similarly, when scrutinizing the examination of Young's modulus in relation to the manufacturer's specified values for ABS-like resin and the results obtained from testing the SLA 3D-printed ABS-like specimens with 100% infill density, a discernible pattern becomes apparent. The SLA 3D-printed ABS-like specimens impressively achieve a striking 99.33% of the values established by the resin manufacturer (Figure 13b). These results underscore the exceptional precision and reliability of SLA 3D printing in producing ABS-like components that closely align with industry standards, demonstrating its suitability for applications demanding consistent and high-quality material performance.

3.3. Comparative Analysis

The comparison of mechanical parameters for the ABS and ABS-like tensile-tested specimens produced through both FDM and SLA 3D printing methods is elucidated in Table 11 and visually represented in Figure 14.

Table 11. Comparison of mechanical parameters in tensile-tested ABS (filament) and ABS-Like (resin) specimens manufactured via FDM and SLA 3D printing.

Material	Case	Average Tensile Strength σ [MPa]	Average Strain ε [%]	Average Nominal Strain at Break ε_{tB} [%]	Average Young's Modulus E [MPa]	Average Maximal Displacement ΔL [mm]	Average Maximal Force at Break F_{max} [N]
ABS (filament)	Case 1 (St. Dev.)	19.507 (0.384)	2.16 (0.04)	2.67 (0.28)	1320.754 (114.695)	3.07 (0.33)	806.355 (22.729)
	Case 2 (St. Dev.)	27.401 (0.756)	2.24 (0.08)	3.62 (0.72)	1788.691 (75.380)	4.16 (0.83)	1093.946 (15.922)
ABS-like (resin)	Case 3 (St. Dev.)	31.517 (3.830)	3.10 (0.75)	3.14 (0.76)	1608.525 (207.890)	6.51 (5.65)	1288.441 (151.859)
	Case 4 (St. Dev.)	45.132 (1.839)	4.15 (0.52)	5.19 (1.15)	2085.842 (66.237)	5.91 (1.32)	1924.241 (77.360)

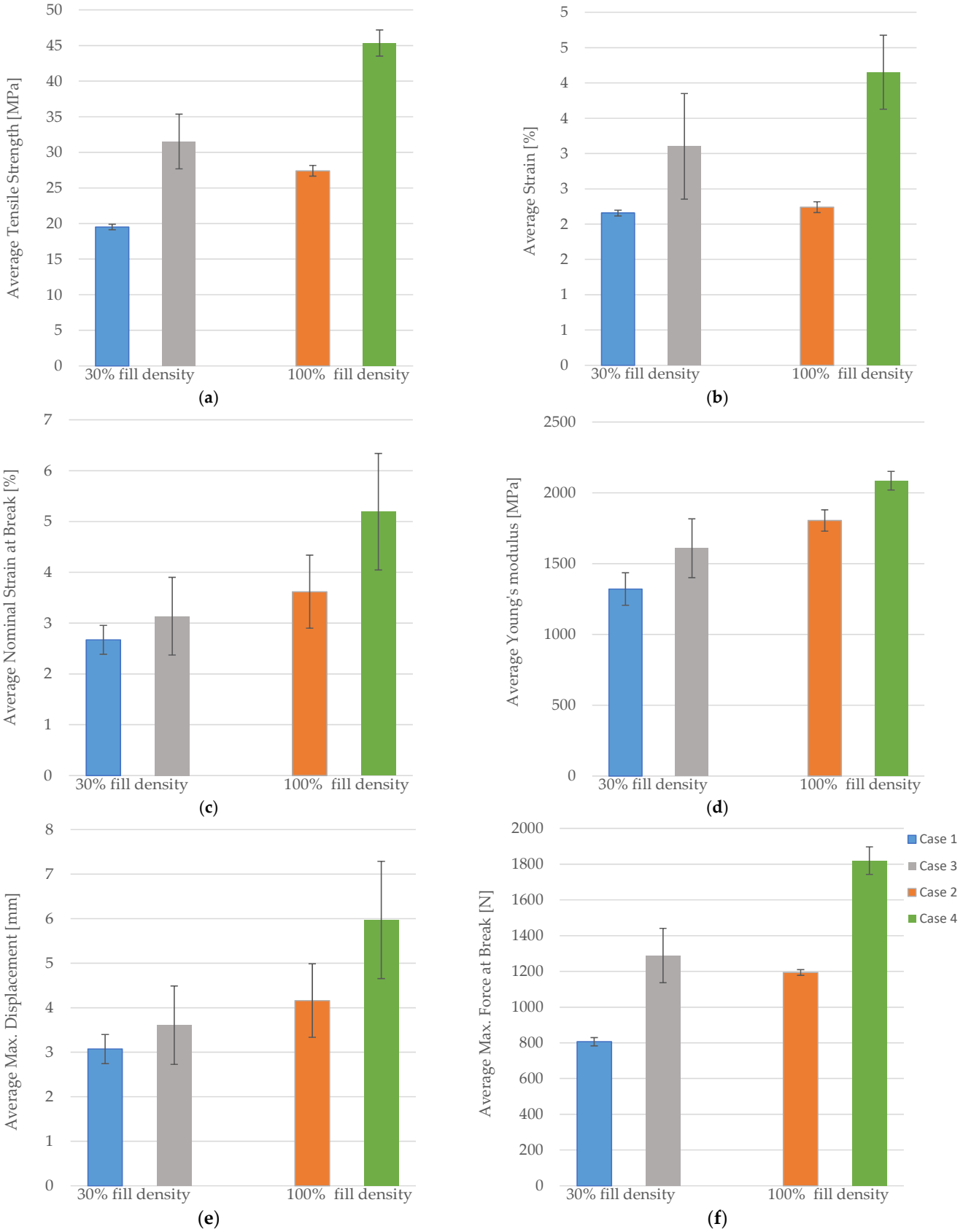


Figure 14. Graphical comparison of mechanical parameters between ABS filament and ABS-like resin: (**a**) average tensile strength, (**b**) average strain, (**c**) average nominal strain at break, (**d**) average Young's modulus, (**e**) average max. displacement, (**f**) average max. force at break.

The results obtained from Table 11 reveal a clear pattern—when 3D-printed using SLA technology, ABS material shows improvements in its specific mechanical parameters, especially in tensile strength, Young's modulus, and displacement.

In the case of SLA 3D-printed ABS-like resin material specimens, which were printed with a 30% infill density, the average tensile strength increased by 38.11% when compared to FDM 3D-printed specimens with a 30% infill density (Figure 14a). For SLA 3D-printed ABS-like resin material specimens with a 100% infill density, the average tensile strength increased by 39.57% compared to FDM 3D-printed specimens with a 100% infill density (Figure 14a).

In the context of SLA 3D-printed ABS-like resin material specimens, printed with a 30% infill density, the average maximum displacement exhibited a 14.96% increase when compared to FDM 3D-printed ABS specimens with a 30% infill density (Figure 14e). In the case of SLA 3D-printed ABS-like resin material specimens with a 100% infill density, the average maximum displacement showed a 30.32% increase compared to FDM 3D-printed ABS specimens with a 100% infill density (Figure 14e).

In the case of SLA 3D-printed ABS-like resin material specimens featuring a 30% infill density, a noteworthy increment of 17.89% in the mean Young's modulus was observed in comparison to their FDM 3D-printed ABS counterparts with a 30% infill density, as illustrated in Figure 14d.

Conversely, for SLA 3D-printed ABS-like resin material specimens featuring a 100% infill density, the average Young's modulus exhibited a noteworthy 13.48% increase when compared to FDM 3D-printed ABS specimens with a full 100% infill density, as also shown in Figure 14c. These observations underscore the benefits of SLA 3D printing in augmenting the mechanical characteristics of ABS-like resin materials, regardless of the infill density, in comparison to FDM printing.

In FDM-printed tensile-tested specimens, those containing ABS material with 30% infill density show an average strain of 2.16%. On the other hand, samples with 100% infill density exhibited a slightly higher deformation, measuring 3.1%. This suggests that increasing the infill density in FDM printing of ABS material does not significantly enhance deformation resistance. In the case of SLA-printed tensile-tested specimens using ABS-like resin with 30% infill density, the average strain is 2.24%. Conversely, tensile-tested specimens with 100% infill density reached a higher strain value of 4.15%. These results indicate that increasing the infill density in SLA printing of ABS-like materials may lead to a substantial increase in deformation, raising questions about the practicality of using higher infill densities (Figure 14b).

The comparison of FDM- and SLA-printed tensile-tested specimens reveals that while higher infill density in FDM does not significantly improve deformation resistance, the same parameter in SLA printing of ABS-like materials may result in a considerable increase in deformation, prompting considerations about the viability of employing elevated infill densities.

Figure 14c furnishes valuable data concerning the average nominal strain at break for both FDM and SLA 3D-printed tensile-tested specimens, considering different infill densities. In the case of FDM-printed specimens with 30% infill density, the average nominal strain at break was recorded at 2.67%, while specimens with 100% infill density exhibited a higher value of 3.62%. This disparity suggests that increasing the infill density in FDM printing has a noticeable impact on the material's ability to withstand strain, resulting in improved performance at higher densities. SLA 3D-printed ABS-like resin samples displayed a different trend. Those with 30% infill density had an average nominal strain at break of 3.614%, whereas specimens with 100% infill density showed a significant increase to 5.19%. This contrast indicates that, unlike FDM, higher infill densities in SLA printing contribute to a substantial rise in the material's ability to endure strain, emphasizing the importance of infill density considerations in material selection and 3D printing processes.

The data presented in Figure 14c highlight the substantial influence of infill density on the average nominal strain at break for FDM and SLA 3D-printed tensile-tested specimens.

The FDM-printed specimens exhibited an observable improvement in strain resistance with increased infill density, while SLA-printed ABS-like resin samples demonstrated a significant rise in strain endurance, underscoring the critical role of infill density considerations in material selection and 3D printing processes.

The average value of the maximum force at failure followed the same trend, as shown in Figure 14f.

Overall, these findings indicate that SLA technology offers clear advantages in terms of mechanical performance, making it a promising option for the production of ABS and ABS-like resin materials with improved mechanical properties.

4. Conclusions

This research has yielded valuable insights into the mechanical properties of 3D-printed ABS filament and ABS-like resin specimens. The two pivotal 3D printing technologies, FDM and SLA, were the principal subjects of inquiry, with a particular focus on their influence on critical mechanical parameters: tensile strength, Young's modulus, and maximum displacement.

The findings illuminate a profound disparity in the mechanical parameters of FDM- and SLA-printed specimens. Notably, SLA consistently emerges as the superior technology, displaying substantial enhancements across the board. Most notably, in the realm of tensile strength, displacement, and Young's modulus, the advantages of SLA technology are strikingly evident.

When ABS samples were evaluated at 100% fill density, a significant increase in average tensile strength was found, namely a 28.81% increase for the 3D printed FDM ABS specimens and a remarkable 30.49% increase for the 3D printed SLA ABS-like resin specimens. In addition, there was also a notable increase in the average maximum displacement value, which increased by 35.51% for the 3D-printed FDM ABS specimens with 100% fill density, while for the SLA 3D-printed ABS-like resins with 100% fill density, the increase in fill density reached an extraordinary 38.92%.

For specimens at 100% fill density, a significant increase in 26.81% was observed for FDM 3D printed ABS and an even more impressive increase in 13.48% for 3D printed ABS-like SLA resin, demonstrating the obvious advantages that SLA has in improving material stiffness.

In a world increasingly shaped by innovation and technological advancement, the significance of these findings cannot be overstated. The implications reach far and wide, extending to industries reliant on 3D-printed components. These discoveries hold the promise of substantially raising the benchmarks for product safety and durability, thereby propelling progress in the fields of manufacturing and design.

In summary, the emergence of SLA technology heralds an exciting frontier, one with the potential to redefine the limits of mechanical performance in 3D-printed ABS and ABS-like resin materials. This narrative extends beyond the confines of the laboratory, casting ripples across various sectors, promising new possibilities and applications with heightened capabilities. The potential of SLA technology paves the way for a brighter future in 3D printing, where the boundaries of what is achievable continue to expand.

The findings suggest promising avenues for future research with the following aims: (1) to investigate how different resin compositions impact mechanical properties for optimized material formulations; (2) to explore the relationship between infill density, resin curing, and mechanical properties to enhance control over deformation characteristics; (3) to extend research to assess the performance of SLA-printed ABS-like resins in diverse applications, providing practical insights, etc. This research framework aims to contribute to the ongoing evolution of 3D printing technologies, unlocking new possibilities for material optimization, application-specific performance, and sustainability in manufacturing processes.

Funding: The APC was funded by University of Novo Mesto, Faculty of Mechanical Engineering, Novo mesto, Slovenia.

Institutional Review Board Statement: Not applicable.

Informed Consent Statement: Not applicable.

Data Availability Statement: The raw data supporting the conclusions of this article will be made available by the authors on request.

Acknowledgments: This research was conducted at the University of Novo Mesto, specifically, within the Faculty of Mechanical Engineering.

Conflicts of Interest: The author declares no conflict of interest.

References

1. Gibson, I.; Rosen, D.; Stucker, B.; Khorasani, M. Introduction and basic principles. In *Additive Manufacturing Technologies*; Gibson, I., Rosen, D., Stucker, B., Khorasani, M., Eds.; Springer: Cham, Switzerland, 2021; pp. 1–21.
2. Snyder, T.J.; Andrews, M.; Weislogel, M.; Moeck, P.; Stone-Sundberg, J.; Birkes, D.; Hoffert, M.P.; Lindeman, A.; Morrill, J.; Fercak, O.; et al. 3D Systems' Technology Overview and New Applications in Manufacturing, Engineering, Science, and Education. *3D Print. Addit. Manuf.* **2014**, *1*, 169–176. [CrossRef] [PubMed]
3. Tofail, S.A.M.; Koumoulos, E.P.; Bandyopadhyay, A.; Bose, S.; O'Donoghue, L.; Charitidis, C. Additive manufacturing: Scientific and technological challenges, market uptake and opportunities. *Mater. Today* **2018**, *21*, 22–37. [CrossRef]
4. *ISO 17296-2:2015*; Additive Manufacturing-General Principles—Part 2: Overview of Process Categories and Feedstock. International Organization for Standardization: Geneva, Switzerland, 2015.
5. Guo, N.; Leu, M.C. Additive manufacturing: Technology, applications and research needs. *Front. Mech. Eng.* **2013**, *8*, 215–243. [CrossRef]
6. *ISO/ASTM 52900:2015*; Additive Manufacturing—General principles—Terminology. ISO/ASTM International: Geneva, Switzerland, 2015.
7. Özsoy, K.; Erçetin, A.; Çevik, Z.A. Comparison of Mechanical Properties of PLA and ABS Based Structures Produced by Fused Deposition Modelling Additive Manufacturing. *Avrupa Bilim Ve Teknol. Derg. (Eur. J. Sci. Technol.)* **2021**, *27*, 802–809. [CrossRef]
8. Jiang, J.; Xu, X.; Stringer, J. Support Structures for Additive Manufacturing: A Review. *J. Manuf. Mater. Process.* **2018**, *2*, 64. [CrossRef]
9. Chua, C.K.; Leong, K.F.; Lim, C.S. *Rapid Prototyping: Principles and Applications*; World Scientific: Singapore, 2010.
10. Algarni, M.; Ghazali, S. Comparative Study of the Sensitivity of PLA, ABS, PEEK, and PETG's Mechanical Properties to FDM Printing Process Parameters. *Crystals* **2021**, *11*, 995. [CrossRef]
11. Mohamed, O.A.; Masood, S.H.; Bhowmik, J.L. Optimization of fused deposition modeling process parameters: A review of current research and future prospects. *Adv. Manuf.* **2015**, *3*, 42–53. [CrossRef]
12. Naveed, N. Investigating the material properties and microstructural changes of fused filament fabricated PLA and tough-PLA parts. *Polymers* **2021**, *13*, 1487. [CrossRef]
13. Jin, Y.; Li, H.; He, Y.; Fu, J. Quantitative analysis of surface profile in fused deposition modelling. *Addit. Manuf.* **2015**, *8*, 142–148. [CrossRef]
14. Dudek, P. FDM 3D printing technology in manufacturing composite elements. *Arch. Metall. Mater.* **2013**, *58*, 1415–1418. [CrossRef]
15. Vyavahare, S.; Teraiya, S.; Panghal, D.; Kumar, S. Fused deposition modelling: A review. *Rapid Prototyp. J.* **2020**, *26*, 176–201. [CrossRef]
16. Hozdić, E.; Hozdić, E. Comparative Analysis of the Influence of Mineral Engine Oil on the Mechanical Parameters of FDM 3D-Printed PLA, PLA+CF, PETG, and PETG+CF. *Materials* **2023**, *16*, 6342. [CrossRef] [PubMed]
17. Zhakeyev, A.; Wang, P.; Zhang, L.; Shu, W.; Wang, H.; Xuan, J. Additive Manufacturing: Unlocking the Evolution of Energy Materials. *Adv. Sci.* **2017**, *4*, 1700187. [CrossRef] [PubMed]
18. Riccio, C.; Civera, M.; Grimaldo Ruiz, O.; Pedullà, P.; Rodriguez Reinoso, M.; Tommasi, G.; Vollaro, M.; Burgio, V.; Surace, C. Effects of Curing on Photosensitive Resins in SLA Additive Manufacturing. *Appl. Mech.* **2021**, *2*, 942–955. [CrossRef]
19. Vaz, V.M.; Kumar, L. 3D Printing as a Promising Tool in Personalized Medicine. *AAPS PharmSciTech* **2021**, *22*, 49. [CrossRef] [PubMed]
20. Taneva, I.; Uzunov, T. Influence of post-polymerization processing on the mechanical characteristics of 3D-printed occlusal splints. *J. Phys. Conf. Ser. IOP Publ.* **2020**, *1492*, 012018. [CrossRef]
21. Manapat, J.Z.; Chen, Q.; Ye, P.; Advincula, R.C. 3D Printing of Polymer Nanocomposites via Stereolithography. *Macromol. Mater. Eng.* **2017**, *302*, 1600553. [CrossRef]
22. Melchels, F.P.W.; Feijen, J.; Grijpma, D.W. A review on stereolithography and its applications in biomedical engineering. *Biomaterials* **2010**, *31*, 6121–6130. [CrossRef]
23. Huang, J.; Qin, Q.; Wang, J. A Review of Stereolithography: Processes and Systems. *Processes* **2020**, *8*, 1138. [CrossRef]

24. Rutkowski, J.V.; Levin, B.C. Acrylonitrile-Butadiene-Styrene Copolymers (ABS): Pyrolysis and Combustion Products and their Toxicity—A review of the Literature. *Fire Mater.* **1986**, *10*, 93–105. [CrossRef]
25. Brown, R.P. Plastics materials. *Polym. Test.* **1988**, *8*, 370. [CrossRef]
26. Padzi, M.M.; Bazin, M.M.; Muhamad, W.M.W. Fatigue Characteristics of 3D Printed Acrylonitrile Butadiene Styrene (ABS). *IOP Conf. Ser. Mater. Sci. Eng.* **2017**, *269*, 012060. [CrossRef]
27. Tan, L.J.; Zhu, W.; Zhou, K. Recent Progress on Polymer Materials for Additive Manufacturing. *Adv. Funct. Mater.* **2020**, *30*, 2003062. [CrossRef]
28. Zhang, H.; Cai, L.; Golub, M.; Zhang, Y.; Yang, X.; Schlarman, K.; Zhang, J. Tensile, creep, and fatigue behaviors of 3D-printed acrylonitrile butadiene styrene. *J. Mater. Eng. Perform.* **2018**, *27*, 57–62. [CrossRef]
29. Gokhare, V.G.; Raut, D.N.; Shinde, D.K. A review paper on 3D-printing aspects and various processes used in the 3D-printing. *Int. J. Innov. Eng. Res. Technol.* **2017**, *6*, 953–958.
30. Alonso, A.; Lázaro, M.; Lázaro, D.; Alvear, D. Thermal characterization of acrylonitrile butadiene styrene-ABS obtained with different manufacturing processes. *J. Therm. Anal. Calorim.* **2023**, *148*, 10557–10572. [CrossRef]
31. Fatimatuzahraa, A.W.; Farahaina, B.; Yusoff, W.A.Y. The effect of employing different raster orientations on the mechanical properties and microstructure of Fused Deposition Modeling parts. In Proceedings of the IEEE Symposium on Business, Engineering and Industrial Applications (ISBEIA), Langkawi, Malaysia, 25–28 September 2011.
32. Sood, A.K.; Ohdar, R.K.; Mahapatra, S.S. Parametric appraisal of mechanical property of fused deposition modelling processed parts. *Mater. Des.* **2010**, *31*, 287–295. [CrossRef]
33. Ziemian, C.; Sharma, M.; Ziemian, S. Anisotropic mechanical properties of ABS parts fabricated by fused deposition modelling. *Mech. Eng.* **2012**, *23*, 159–180.
34. Ziemian, S.; Okwara, M.; Ziemian, C.W. Tensile and fatigue behavior of layered acrylonitrile butadiene styrene. *Rapid Prototyp. J.* **2015**, *21*, 270–278. [CrossRef]
35. Rankouhi, B.; Javadpour, S.; Delfanian, F.; Letcher, T. Failure Analysis and Mechanical Characterization of 3D Printed ABS With Respect to Layer Thickness and Orientation. *J. Fail. Anal. Prev.* **2016**, *16*, 467–481. [CrossRef]
36. Nomani, J.; Wilson, D.; Paulino, M.; Mohammed, M.I. Effect of layer thickness and cross-section geometry on the tensile and compression properties of 3D printed ABS. *Mater. Today* **2020**, *22*, 100626. [CrossRef]
37. Suaidi, S.N.S.W.; Azizul, M.A.; Sulaiman, S.; Hao, T.Y. Effect of fused deposition modelling process parameters on the quality of ABS product. *J. Ind. Eng. Innov.* **2020**, *2*, 9.
38. Baich, L.; Manogharan, G.; Marie, H. Study of infill print design on production cost-time of 3D printed ABS parts. *Int. J. Rapid Manuf.* **2016**, *5*, 308–319. [CrossRef]
39. Yadav, D.; Chhabra, D.; Garg, R.K.; Ahlawat, A.; Phagat, A. Optimization of FDM 3D printing process parameters for multi-material using artificial neural network. *Mater. Today Proc.* **2020**, *21*, 1583–1591. [CrossRef]
40. Samykano, M.; Selvamani, S.K.; Kadirgama, K.; Ngui, W.K.; Kanagaraj, G.; Sudhakar, K. Mechanical property of FDM printed ABS: Influence of printing parameters. *Int. J. Adv. Manuf. Technol.* **2019**, *102*, 2779–2796. [CrossRef]
41. Rodríguez-Panes, A.; Claver, J.; Camacho, A.M. The Influence of Manufacturing Parameters on the Mechanical Behaviour of PLA and ABS Pieces Manufactured by FDM: A Comparative Analysis. *Materials* **2018**, *11*, 1333. [CrossRef] [PubMed]
42. Abbott, A.C.; Tandon, G.P.; Bradford, R.L.; Koerner, H.; Baur, J.W. Process-structure-property effects on ABS bond strength in fused filament fabrication. *Addit. Manuf.* **2018**, *19*, 29–38. [CrossRef]
43. Guimarães, A.L.A.; Neto, V.G.; Foschini, C.R.; Azambuja, M.D.A.; Hellmeister, L.A.V. Influence of ABS print parameters on a 3D open-source, self-replicable printer. *Rapid Prototyp. J.* **2020**, *26*, 1733–1738. [CrossRef]
44. Domingo-Espin, M.; Travieso-Rodriguez, J.A.; Jerez-Mesa, R.; Lluma-Fuentes, J. Fatigue Performance of ABS Specimens Obtained by Fused Filament Fabrication. *Materials* **2018**, *11*, 2521. [CrossRef]
45. Galeja, M.; Hejna, A.; Kosmela, P.; Kulawik, A. Static and Dynamic Mechanical Properties of 3D Printed ABS as a Function of Raster Angle. *Materials* **2020**, *13*, 297. [CrossRef]
46. Yankin, A.; Alipov, Y.; Temirgali, A.; Serik, G.; Danenova, S.; Talamona, D.; Perveen, A. Optimization of Printing Parameters to Enhance Tensile Properties of ABS and Nylon Produced by Fused Filament Fabrication. *Polymers* **2023**, *15*, 3043. [CrossRef] [PubMed]
47. Golubović, Z.; Danilov, I.; Bojović, B.; Petrov, L.; Sedmak, A.; Mišković, Ž.; Mitrović, N. A Comprehensive Mechanical Examination of ABS and ABS-like Polymers Additively Manufactured by Material Extrusion and Vat Photopolymerization Processes. *Polymers* **2023**, *15*, 4197. [CrossRef]
48. Wypych, G. Odor in Relation to Different Polymers. In *Handbook of Odors in Materials*; Elsevier: Amsterdam, The Netherlands, 2013; pp. 73–99.
49. Campo, E.A. *Selection of Polymeric Materials—How to Select Design Properties from Different Standards*; William Andrew Inc.: Norwich, NY, USA, 2008; ISBN 978-0-8155-1551-7 (978-0-8155).
50. Zhu, Z.H.; Zhang, N.; Wang, T.; Hao, M.Y. Short Review of Polymer Composites for 3D Printing. *IOP Conf. Ser. Mater. Sci. Eng.* **2020**, *758*, 012046. [CrossRef]
51. Poyraz, O. Influence of Build Direction and Post Processes on the Material and Part Attributes of Hard Resins Fabricated by Photopolymerization Based Additive Manufacturing. *Mater. Res.* **2023**, *26*, e20220362. [CrossRef]

52. Billings, C.; Cai, C.; Liu, Y. Utilization of Antibacterial Nanoparticles in Photocurable Additive Manufacturing of Advanced Composites for Improved Public Health. *Polymers* **2021**, *13*, 2616. [CrossRef] [PubMed]
53. Markiz, N.; Horváth, E.; Ficzer, P. Influence of printing direction on 3D printed ABS specimens. *Prod. Eng. Arch.* **2020**, *26*, 127–130. [CrossRef]
54. Anastas, P.T.; Hammond, D.G. *Inherent Safety at Chemical Sites—Reducing Vulnerability to Accidents and Terrorism through Green Chemistry*; Elsevier Inc.: Amsterdam, The Netherlands, 2016; ISBN 978-0-12-804190-1.
55. 3DTRCEK. Available online: https://3dtrcek.si/sl/abs-flame-retardant-v0-filament (accessed on 17 October 2023).
56. ANYCUBIC. Available online: https://www.anycubic.com/collections/abs-like-resin/products/get-3-for-the-price-of-2-anycubic-abs-like-resin (accessed on 17 October 2023).
57. *ISO 527-2:2012*; Plastics-Determination of Tensile Properties—Part 2: Test Conditions for Moulding and Extrusion Plastics. International Organization for Standardization: Geneva, Switzerland, 2012.

Disclaimer/Publisher's Note: The statements, opinions and data contained in all publications are solely those of the individual author(s) and contributor(s) and not of MDPI and/or the editor(s). MDPI and/or the editor(s) disclaim responsibility for any injury to people or property resulting from any ideas, methods, instructions or products referred to in the content.